Active Noise Control Based on State Feedback by a Concentrated Mass Model

Shotaro HISANO[1]; Satoshi ISHIKAWA[2]; Shinya KIJIMOTO[3]; Yosuke KOBA[4]

[1,2,3,4]Kyushu University, Japan

ABSTRACT

We herein propose a new model-based control method, in place of traditional adaptive control, for a low-frequency noise problem in a closed space. The proposed control method is based on state feedback control and a model of the acoustic space obtained by the concentrated mass model. Thus, we can control noise in the entire space. According to the concentrated mass model, the acoustic space is modeled as masses, connecting linear springs, connecting dampers, and base support dampers. Furthermore, a loudspeaker, as a control source, is also modeled by a mass, a spring, and a damper. In the present paper, as a first step, we constructed a coupled analysis model of a one-dimensional sound field and the loudspeaker. We designed the model-based system for the standing sound wave in the low-frequency band. Specifically, we realized a state feedback control system based on a Kalman filter and pole placement. Modal reduction using modal analysis is conducted to reduce the computation time of the controller. Then, we conducted experiments and a numerical simulation of the one-dimensional sound tube to confirm the validity of the analysis model. Moreover, we perform an experiment to control the noise in the sound tube. The noise is reduced around the resonance frequency in the entire space. Therefore, the proposed method is valid for noise control in a closed space.

Keywords: Active noise control, Model-based control, Modeling, State feedback, Concentrated mass model, Modal analysis

1. INTRODUCTION

Several adaptive control methods have been proposed in conventional research on active noise control (1). However, it is difficult for these methods to control noise in a large sound space. In a closed space, controlling noise in the entire acoustic space requires proper placement of the microphones and loudspeakers. Their placement is determined empirically based on experimental results because there are no placement guidelines (2). However, we can control the entire acoustic space using system theory if we model the acoustic space and the acoustic device as a system equation. Therefore, a method of active noise control using the system equation of the finite element method was proposed (3). However, a confirmatory experiment was not conducted, and coupling of the acoustic space and loudspeakers was not considered. On the other hand, the method of using experimental modal analysis considers the dynamics of the loudspeakers (4). However, measurement of the frequency response is required in advance. Based on the above considerations, theoretical modeling of the acoustic space and the loudspeakers and the establishment of a practical control method are necessary.

In the present study, we model the acoustic space as the concentrated mass model, which consists of masses, connecting linear springs, connecting dampers, and base support dampers (5). In addition, a loudspeaker, as an actuator, is modeled by a mass, a spring, and a damper. We model the coupling of the acoustic space and the loudspeaker. Furthermore, we design a model-based control system using the coupled model and the state feedback to control noise in the entire acoustic space. In the present paper, as a first step, we deal with the one-dimensional sound field. We constructed an analysis model

[1] s.hisano@sky.mech.kyushu-u.ac.jp
[2] ishikawa@mech.kyushu-u.ac.jp
[3] kiji@mech.kyushu-u.ac.jp
[4] koba@mech.kyushu-u.ac.jp

of the sound field and the loudspeaker, and we designed a model-based control system for steady-state sound waves below 500 Hz. The state feedback control system is designed based on a Kalman filter and pole placement. Then, we conducted experiments and a numerical simulation of a one-dimensional sound tube in order to confirm the validity of the analysis model. In addition, we designed the control system and performed an experiment to control the noise in the sound tube.

2. MODELING OF THE ACOUSTIC SPACE/LOUDSPEAKER COUPLED SYSTEM

In the present paper, we consider a one-dimensional acoustic problem in a cylindrical tube, as shown Fig. 1. A speaker is installed at each end of the cylindrical tube. The left speaker is the noise source, and the right speaker is the actuator. Then, the control input is calculated from the sound pressure as measured by the microphones placed at a distance L_m from the right end of the tube. In this section, we model the coupled system of the acoustic space and the loudspeaker, as a concentrated mass model.

2.1 Modeling of Acoustic Space Using a Concentrated Mass Model

In this section, we model acoustic problems in a cylindrical tube using the concentrated mass model (5). The air is modeled as masses, connecting linear springs, connecting dampers, and base support dampers, as shown in Fig. 2. The air is divided into N elements, each element having a length *l* in the tube, as shown Fig. 1, where *L* is the pipe length, and *D* is the diameter of the pipe. The mass is concentrated on the nodal points. Then, the mass at each nodal point, m, is given as follows:

$$m = \rho A l \tag{1}$$

where ρ is the density of air in the equilibrium state, and A is the cross-sectional area of cylindrical tube. In addition, x_i is the displacement of the nodal point i and p_i is the pressure in element i. Assuming an adiabatic process in element i, the sound pressure, dp_i, is given as follows using the relative displacement of element i, $x_j - x_{j-1}$ (5):

$$dp_i = -\frac{k\left(x_i - x_{i-1}\right)}{A} \tag{2}$$

where k is the coefficient of the connecting spring. The pressure in the equilibrium state is p_0 and the specific heat ratio of the air is γ. Then, k is given as follows:

$$k = \frac{p_0 A \gamma}{l} \tag{3}$$

In this paper, the coefficient of the base support damper, c^b, and the coefficient of the connecting damper, c^c, are determined experimentally.

2.2 Modeling the Electro-dynamic Type Loudspeaker

In this section, we model the loudspeaker shown in Fig. 3(a). The loudspeaker is assumed to be a circular baffle having equivalent diameter D_s when the loudspeaker is used in a low-frequency domain of less than 1000 Hz (6). Then, the dynamics of the loudspeaker affected by the sound pressure can be expressed by an equivalent circuit, as shown in Fig. 3(b). In Fig. 3(b), the left side circuit is the driver circuit of a coil, and the right side circuit is the equivalent circuit derived from the mechanical behavior of the vibration board. The equation of motion in the frequency domain is given by

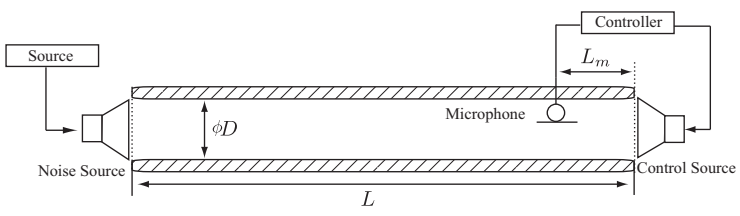

Figure 1 – Control system and control object

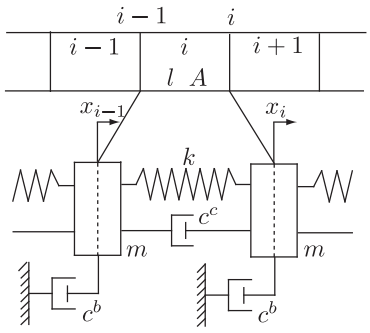

Figure 2 – Concentrated mass model

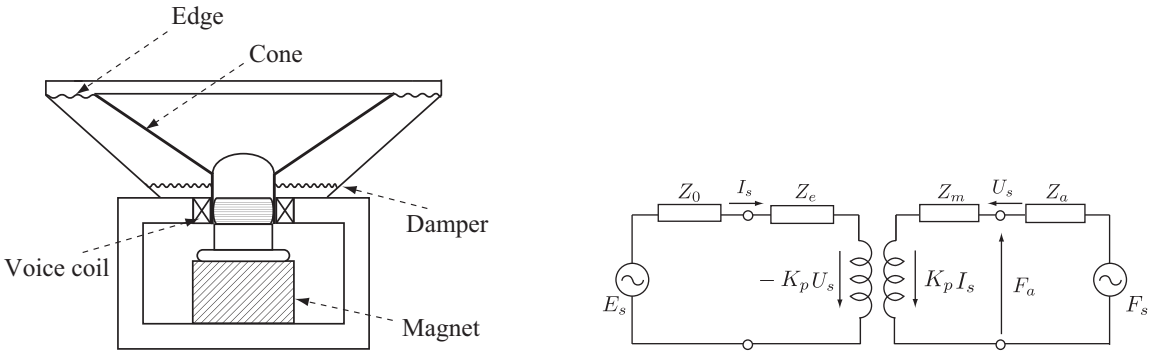

(a) Sectional view (b) Equivalent circuit

Figure 3 – The loudspeaker of electro dynamic type

$$(Z_m + Z_a)U_s - K_p I_s = F_s \tag{4}$$

$$(Z_e + Z_0)I_s + K_p U_s = E_s \tag{5}$$

where U_s is the velocity of the vibration board, I_s is the current in the voice coil, F_s is the vibratory force of the external sound sources in the acoustic field, E_s is the voltage applied to the loudspeaker, K_p is the power factor, Z_a is the mechanical impedance for the external source, Z_a is the mechanical impedance for the voice circuit, Z_a is the electrical impedance of the voice circuit, and Z_a is the electrical impedance. These impedances are given as follows (6):

$$Z_m = j\omega m_s + c_s + \frac{k_s}{j\omega} \tag{6}$$

$$Z_e + Z_0 = r_s + j\omega L_s \tag{7}$$

where m_s is the mass of the vibration board, c_s is the mechanical damper of the loudspeaker, k_s is the mechanical stiffness, r_s is the sum of the voice coil resistance and the internal resistance, L_s is the inductance of the voice coil, $j = \sqrt{-1}$, and ω is the angular frequency. The force acting on the vibration board from the air is given by

$$F_a = F_s - Z_a U_s \tag{8}$$

Equations (4) and (5) are given as follows in the time domain using Eqs. (6), (7) and (8):

$$\left.\begin{aligned} m_s\ddot{x}_s + c_s\dot{x}_s + k_s x_s &= f_a + K_p i_s \\ L_s\dot{i}_s + r_s i_s &= e_s - K_p\dot{x}_s \end{aligned}\right\} \tag{9}$$

where x_s is the displacement of the vibration board, i_s is the current in the voice coil, f_a is the force that the vibration board receives from the air, e_s is the voltage applied to the voice coil, and all are functions of time. The first equation of Eq. (9) is the equation of motion of the vibration board. The force $K_p i_s$ is generated by the current in the drive coil, and the force f_a is generated by the air. The second equation of Eq. (9) is the equation of the electrical circuit. The electromotive force is generated by the vibration of the vibration board and the input voltage is applied to the voice coil. Since the time constant $\tau = L_s / r_s$ can be neglected in the low-frequency range, we can neglect the first term on the left-hand side of the second equation of Eq. (9). Then, Eq. (9) can be simplified as follows:

$$m_s\ddot{x}_s + c_s'\dot{x}_s + k_s x_s = f_a + K_s e_s \tag{10}$$

where $K_s = K_p / r_s$ is the factor that converts the force to the voltage, and $c_s' = c_s + K_p K_s$. Equation (10) express the loudspeaker as the dynamic model in Fig. 4.

2.3 Modeling of the Boundary of Acoustic Space and the Loudspeaker

In this section, we model the boundary of the acoustic space and the loudspeaker. We consider the case in which the equivalent cross-sectional area of the vibration board of the left speaker, A_s, is smaller than the cross-sectional area of the cylindrical tube, A, as shown in Fig. 5, in which x_s is the displacement of the vibration board of the loudspeaker, and x_1 is the displacement of the mass point 1 of the air next to the vibration board. From adiabatic change, the pressure variation in the boundary (element 1) is given by

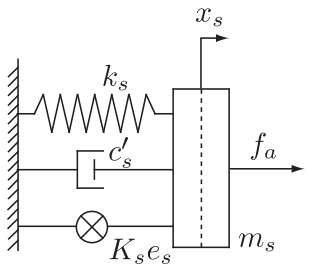

Figure 4 – Equivalent mass of the loudspeaker

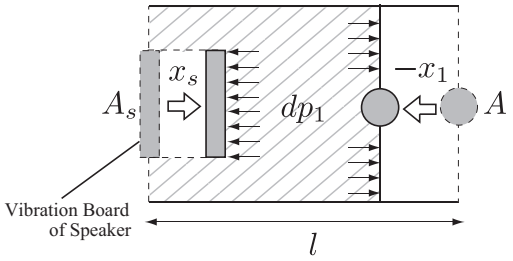

Figure 5 – Boundary condition of the left end

$$dp_1 = \frac{p_0 (Al)^{\gamma}}{(Al + Ax_1 - A_s x_s)^{\gamma}} - p_0 \tag{11}$$

Linearizing Eq. (11) in the vicinity of p_0, we obtain

$$dp_1 = -\frac{p_0 \gamma}{Al}(Ax_1 - A_s x_s) \tag{12}$$

The force acting on the vibration board, f_{a1}^L, and the force acting on the mass point of the right, f_{a1}^R, by the sound pressure, dp_1, are given as follows:

$$\left.\begin{aligned} f_{a1}^L &= -dp_1 A_s \\ f_{a1}^R &= -dp_1 A \end{aligned}\right\} \tag{13}$$

When we analyze the loudspeaker, we use the force generated by the air, where $f_a = f_{a1}^L$ in Eqs. (9) and (10). In addition, we model the boundary at the right end (element N) in the same manner.

3. Control System Design

In this section, we design a control system for the acoustic space using the proposed analysis model in Section 2. First, we deform the coupled system to the system equation. Next, we conduct model reduction to reduce the computation time of the controller. In addition, we design an observer-based controller using a Kalman filter and pole placement design.

3.1 System Equation of the Coupled System

We model the coupled system in Fig. 1 as a concentrated mass model of $n\,(=N+2)$ degrees of freedom, as shown in Fig. 6. The acoustic space is divided into *N* elements. Subscripts s1 and s2 indicate that variables are associated with the left and right speakers, respectively. The displacement vector is defined as follows:

$$\boldsymbol{x} = \begin{bmatrix} x_{s1} & x_{s2} & x_1 & \cdots & x_N \end{bmatrix}^T \tag{14}$$

The equation of motion of a coupled system becomes

$$\boldsymbol{M}\ddot{\boldsymbol{x}} + \boldsymbol{C}\dot{\boldsymbol{x}} + \boldsymbol{K}\boldsymbol{x} = \boldsymbol{G}d + \boldsymbol{H}u \tag{15}$$

where $\boldsymbol{M} \in \mathrm{R}^{n \times n}$ is the mass matrix of the coupled system, $\boldsymbol{C} \in \mathrm{R}^{n \times n}$ is the damping matrix, $\boldsymbol{K} \in \mathrm{R}^{n \times n}$ is the stiffness matrix, $\boldsymbol{G} \in \mathrm{R}^{n \times 1}$ is the position at which the noise is acting, and $\boldsymbol{H} \in \mathrm{R}^{n \times 1}$ is the position at which the input is acting. Positions $\boldsymbol{G}$ and $\boldsymbol{H}$ are given as follows:

$$\left.\begin{aligned} \boldsymbol{G} &= \begin{bmatrix} 1 & 0 & 0 & \cdots & 0 \end{bmatrix}^T \\ \boldsymbol{H} &= \begin{bmatrix} 0 & 1 & 0 & \cdots & 0 \end{bmatrix}^T \end{aligned}\right\} \tag{16}$$

If we define the state vector as $\boldsymbol{q} = \begin{bmatrix} \boldsymbol{x}^T & \dot{\boldsymbol{x}}^T \end{bmatrix}^T$, Eq. (15) becomes

$$\left.\begin{aligned} \dot{\boldsymbol{q}} &= \boldsymbol{A}\boldsymbol{q} + \boldsymbol{B}u + \boldsymbol{D}d \\ y &= \boldsymbol{C}_o \boldsymbol{q} \end{aligned}\right\} \tag{17}$$

In Eq. (18), each matrix is written as follows:

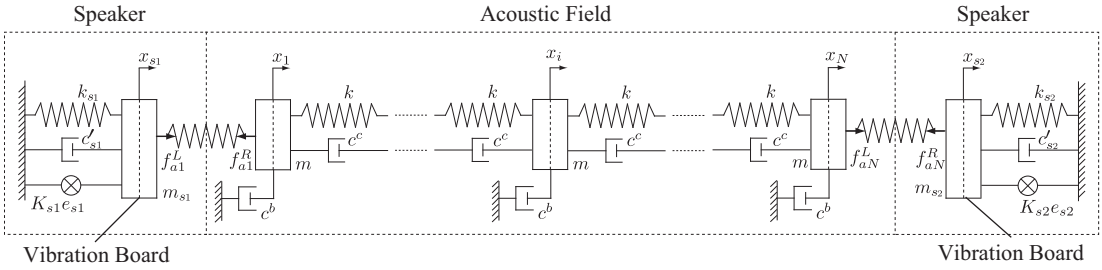

Figure 6 – Coupled system of a loudspeaker and a concentrated mass model

$$\left.\begin{aligned} \boldsymbol{A} &= \begin{bmatrix} \boldsymbol{0}_{n\times n} & \boldsymbol{I}_{n\times n} \\ -\boldsymbol{M}^{-1}\boldsymbol{K} & -\boldsymbol{M}^{-1}\boldsymbol{C} \end{bmatrix}, \quad \boldsymbol{B} = \begin{bmatrix} \boldsymbol{0}_{n\times 1} \\ \boldsymbol{M}^{-1}\boldsymbol{G} \end{bmatrix} \\ \boldsymbol{D} &= \begin{bmatrix} \boldsymbol{0}_{n\times 1} \\ \boldsymbol{M}^{-1}\boldsymbol{H} \end{bmatrix}, \quad \boldsymbol{C}_o = \begin{bmatrix} 0 & 0 & 0 & \cdots & 0 & \underbrace{-1}_{j-1} & \underbrace{1}_{j} & 0 & \cdots & 0 & \boldsymbol{0}_{1\times n} \end{bmatrix} \end{aligned}\right\} \tag{18}$$

where j is the element number of the observation point, and $\boldsymbol{C}_o$ is derived from the fact that the sound pressure, dp_j, is proportional to the relative displacement $x_j - x_{j-1}$.

3.2 Model Reduction

The *n*-degree-of-freedom vibration system is reduced using modal coordinates $\boldsymbol{\eta}$. The modal coordinates vector $\boldsymbol{\eta}$ is defined as

$$\boldsymbol{\eta} = \begin{bmatrix} \eta_1 & \cdots & \eta_n & \dot{\eta}_1 & \cdots & \dot{\eta}_n \end{bmatrix}^T \tag{19}$$

The state vector using the physical coordinate $\boldsymbol{q}$ is given by

$$\boldsymbol{q} = \boldsymbol{S}\boldsymbol{\eta} \tag{20}$$

where $\boldsymbol{S}$ is given as follows:

$$\boldsymbol{S} = \begin{bmatrix} \boldsymbol{\Phi} & \boldsymbol{0} \\ \boldsymbol{0} & \boldsymbol{\Phi} \end{bmatrix} \tag{21}$$

$\boldsymbol{\Phi} = \begin{bmatrix} \phi_1 & \phi_2 & \cdots & \phi_n \end{bmatrix} \in \mathrm{R}^{n\times n}$ is the modal matrix derived from Eq. (15) when $\boldsymbol{C}$, d, and u are neglected. ϕ_i is the *i*-th eigenvector. If the noise source is neglected ($d = 0$) in Eq. (17), the state equation using the mode coordinate $\boldsymbol{\eta}$ can be expressed as follows:

$$\left.\begin{aligned} \dot{\boldsymbol{\eta}} &= \bar{\boldsymbol{A}}\boldsymbol{\eta} + \bar{\boldsymbol{B}}u \\ \bar{y} &= \bar{\boldsymbol{C}}_o\boldsymbol{\eta} \end{aligned}\right\} \tag{22}$$

where

$$\left.\bar{\boldsymbol{A}} = \boldsymbol{S}^{-1}\boldsymbol{A}\boldsymbol{S}, \quad \bar{\boldsymbol{B}} = \boldsymbol{S}^{-1}\boldsymbol{B} \quad \bar{\boldsymbol{C}}_o = \boldsymbol{C}_o\boldsymbol{S}\right\} \tag{23}$$

and $\boldsymbol{\Phi}$ is normalized as $\boldsymbol{\Phi}^T\boldsymbol{M}\boldsymbol{\Phi} = \boldsymbol{I}_{\bar{n}\times\bar{n}}$. Then, the first through $\bar{n}$-th order modes remain, and the higher-order modes are neglected. The reduced modal coordinates vector $\boldsymbol{\eta}_{\bar{n}}$ is defined as

$$\boldsymbol{\eta}_{\bar{n}} = \begin{bmatrix} \eta_1 & \cdots & \eta_{\bar{n}} & \dot{\eta}_1 & \cdots & \dot{\eta}_{\bar{n}} \end{bmatrix}^T \tag{24}$$

The reduced order system is given as follows using Eq. (24)[Consider replacing by "$\boldsymbol{\eta}_{\bar{n}}$".]:

$$\left.\begin{aligned} \dot{\boldsymbol{\eta}}_{\bar{n}} &= \bar{\boldsymbol{A}}_{\bar{n}}\boldsymbol{\eta}_{\bar{n}} + \bar{\boldsymbol{B}}_{\bar{n}}u \\ \bar{y}_{\bar{n}} &= \bar{\boldsymbol{C}}_{o\bar{n}}\boldsymbol{\eta}_{\bar{n}} \end{aligned}\right\} \tag{25}$$

3.3 Design of the Controller

We design the controller based on Eq. (25). In the present paper, we use the Kalman filter to estimate the quantity of the state (the number of microphones are r). According to the theory of the Kalman filter (7), the estimated state vector, $\hat{\boldsymbol{\eta}}_{\bar{n}}$, is given by

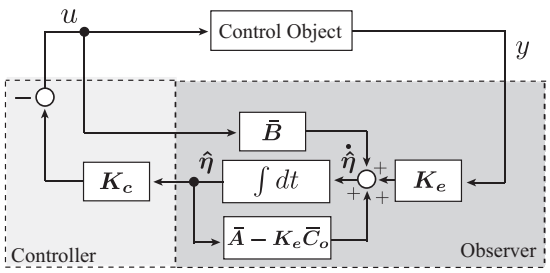

Figure 7 – Block diagram of the control system

$$\dot{\hat{\boldsymbol{\eta}}}_{\bar{n}} = \left(\bar{\boldsymbol{A}}_{\bar{n}} - \boldsymbol{K}_e \bar{\boldsymbol{C}}_{o\bar{n}}\right)\hat{\boldsymbol{\eta}}_{\bar{n}} + \bar{\boldsymbol{B}}_{\bar{n}} u + \boldsymbol{K}_e y \tag{26}$$

where the Kalman gain $\boldsymbol{K}_e \in \mathrm{R}^{r\times 2\bar{n}}$ is $\boldsymbol{K}_e = \boldsymbol{P}\bar{\boldsymbol{C}}_{o\bar{n}}^T \boldsymbol{R}^{-1}$, in which $\boldsymbol{P} \in \mathrm{R}^{2\bar{n}\times 2\bar{n}}$ is obtained by solving the Riccati algebraic equation:

$$\bar{\boldsymbol{A}}_{\bar{n}}\boldsymbol{P} + \boldsymbol{P}\bar{\boldsymbol{A}}_{\bar{n}}^T - \boldsymbol{P}\bar{\boldsymbol{C}}_{o\bar{n}}^T \boldsymbol{R}^{-1}\bar{\boldsymbol{C}}_{o\bar{n}}\boldsymbol{P} + \boldsymbol{Q} = 0 \tag{27}$$

where $\boldsymbol{Q} \in \mathrm{R}^{2\bar{n}\times 2\bar{n}}$ is the covariance matrix of system noise, and $\boldsymbol{R} \in \mathrm{R}^{r\times r}$ is the covariance matrix of the observation noise.

The controller from the state feedback (8) can be written as follows:

$$\left.\begin{aligned} \dot{\hat{\boldsymbol{\eta}}}_{\bar{n}} &= \boldsymbol{K}_e y + \left(\bar{\boldsymbol{A}}_{\bar{n}} - \boldsymbol{K}_e \bar{\boldsymbol{C}}_{o\bar{n}} - \bar{\boldsymbol{B}}_{\bar{n}}\boldsymbol{K}_c\right)\hat{\boldsymbol{\eta}}_{\bar{n}} \\ u &= -\boldsymbol{K}_c \hat{\boldsymbol{\eta}}_{\bar{n}} \end{aligned}\right\} \tag{28}$$

where the feedback gain $\boldsymbol{K}_c \in \mathrm{R}^{2n\times 1}$ is obtained by the solution of the pole placement problem. We move the poles of the system as desired using Ackermann's formula (8). Figure 7 shows a block diagram of the control system in Eq. (28).

4. VALIDITY OF THE ANALYSIS MODEL

In this section, we verify the validity of the analysis model proposed in Section 2. We first compare the numerical results obtained using Eqs. (9) and (10) and the measurement results for the vibration of the loudspeaker in order to confirm the validity of the loudspeaker equation. In addition, we measured the sound pressure in the acoustic tube when the noise is generated from the left speaker in Fig. 9. We compare the numerical results using Eq. (17) with the experimental results to confirm the validity of the coupled analysis model.

4.1 Validity of the Loudspeaker Model

In this section, we measured the vibration of the loudspeaker without the tube in order to confirm the validity of Eq. (10). We used a Fostex FF85WK loudspeaker. The parameters of the loudspeaker were obtained from the specifications listed in Table 1. We calculated the frequency response of the displacement of the vibration board using Eqs. (9) and (10). Figure 8 shows the experimental and numerical results. The input to the loudspeaker was a sine wave with voltage amplitude $\delta_e = 0.1[V]$ in each frequency. The numerical results obtained by Eqs. (9) and (10) are in good agreement, so the simple Eq. (10) is valid in the low-frequency domain. Moreover, the experimental and numerical results are in good agreement. The difference between Eqs. (9) and (10) appears at high frequencies in the phase. We can use Eq. (10) because we consider the frequency range of less than 500 Hz.

4.2 Validity of the Coupled Analysis Model

We compare the experimental results of the sound tube in Fig. 9 with the numerical results obtained by the concentrated mass model when the control input is zero in order to confirm the validity of the coupled analysis model of the loudspeaker and the acoustic space. The experiment is performed in an anechoic camber room. The parameters of the experimental equipment are listed in Tables 1 and 2.

The numerical calculation using the concentrated mass model is performed by numerical integration using Eq. (17). The numerical integration is by the Runge-Kutta method with a time interval of 1/100,000 [s] and 200 partitions in the air region. The parameters of the analysis are listed

in Tables 1 and 2. The coefficient of the base support damper and the coefficient of the connecting damper are set to match the peak value at the fifth-order resonance frequency. The input voltage to the left speaker, as the noise source, is given by the following equation:

$$e_{s1} = \delta_e \sin \omega t \tag{29}$$

where ω is the frequency of the input voltage. The frequency is less than 500 Hz.

Table 1 – Parameters of the loudspeaker (FF85WK)

D_s[mm]	60.0	$r_s[\Omega]$	7.2
m_s [kg]	0.00211	L_s[m H]	0.032
k_s[N/m]	1100.11	K_p[N/ A]	3.93
c_s [N/m^2]	0.5		

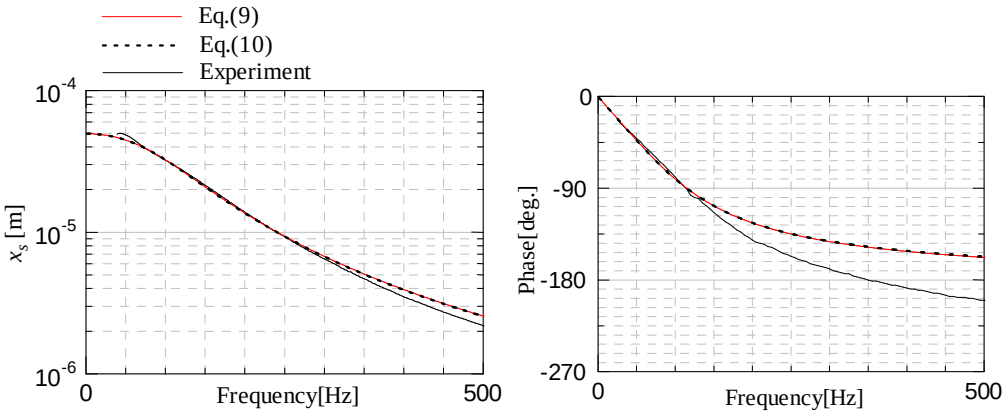

Figure 8 – Frequency response of the loudspeaker

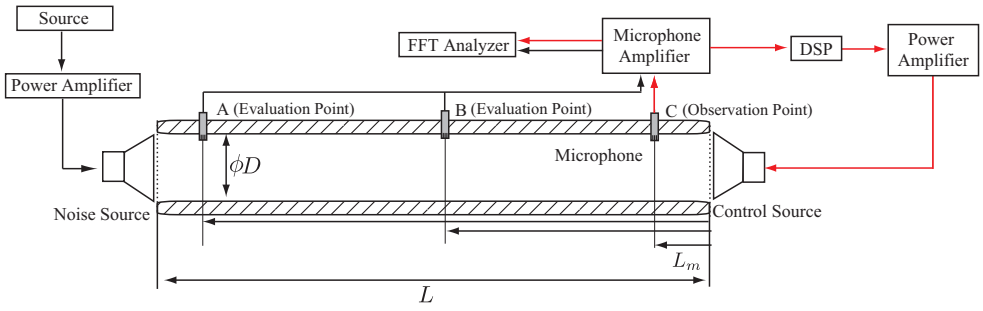

Figure 9 – Experimental equipment used to confirm the effectiveness of the proposed control system

Table 2 – Parameters of the experimental equipment

L[m]	2.0	γ	1.4
D[mm]	77.0	c^c [N/m^2]	0.03
p_0[kPa]	101.3	c^b [N/m^2]	0.0018
ρ[kg/ m^3]	1.1926	δ_e[V]	0.1

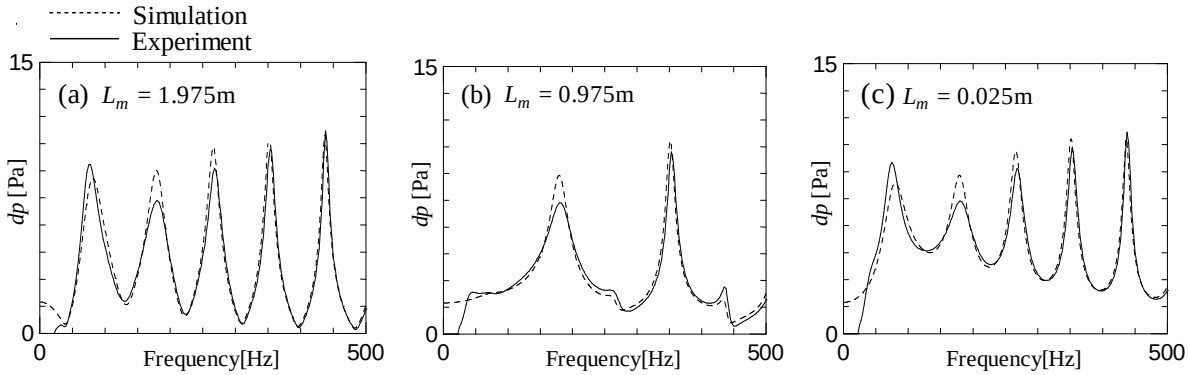

Figure 10 – Frequency response of pressure in the one-dimension sound tube

The results are shown in Fig. 10. The frequency response of the sound pressure is shown in Fig. 10(a) (microphone position: $L_m = 1.975$[m]), Fig. 10(b) ($L_m = 0.975$[m]), and Fig. 10(c) ($L_m = 0.025$[m]). The dashed lines indicate the numerical results, and the solid lines indicate the experimental results. The experimental and numerical results are in good agreement at each microphone position. Some of the peak values of the numerical results do not agree with the peak value of the experimental results, because the damper of the concentrated mass model is not optimized. In this regard, the analysis accuracy can be further improved by setting the damping to be optimal. Based on the above considerations, the coupled analysis model is valid.

5. VALIDITY OF THE CONTROL SYSTEM

In this section, we verify the control effect using the controller by Eq. (28). Therefore, we give the noise to the left speaker and we give the control input to the right speaker, as shown in Fig. 9. Then, the sound pressure is measured in the acoustic tube when the control is executed to confirm the control effect.

5.1 Control System

We conducted a noise control experiment to confirm the control effect of the controller of Eq. (28). Figure 9 shows the experimental equipment. The control input is sent to the right speaker, and a sine wave is sent to the left speaker as noise. Then, we perform the noise control of the first through 7-th mode ($\bar{n} = 7$). Note, the control input is calculated by the DSP (sBOX-C6713 by MTT Corporation). The observation value is the only the sound pressure measured at the microphone C ($L_m = 0.025$[m]), and the other microphones (A, B) are used for the evaluation of the control effect. In addition, discretizing Eq. (28) as the following digital control system (9):

$$\left.\begin{aligned} \hat{\boldsymbol{\eta}}_{\bar{n}}[i+1] &= \boldsymbol{A_d}\hat{\boldsymbol{\eta}}_{\bar{n}}[i] + \boldsymbol{B_d}u[i] + \boldsymbol{H_d}y[i] \\ u[i] &= -\boldsymbol{K}_c\hat{\boldsymbol{\eta}}_{\bar{n}}[i] \end{aligned}\right\} \tag{30}$$

where

$$\begin{aligned} \boldsymbol{A_d} &= e^{(\bar{\boldsymbol{A}}_{\bar{n}} - \boldsymbol{K}_e\bar{\boldsymbol{C}}_{o\bar{n}})T} \\ \boldsymbol{B_d} &= \int_0^T e^{(\bar{\boldsymbol{A}}_{\bar{n}} - \boldsymbol{K}_e\bar{\boldsymbol{C}}_{o\bar{n}})\tau} d\tau \cdot \bar{\boldsymbol{B}}_{\bar{n}} \\ \boldsymbol{H_d} &= \int_0^T e^{(\bar{\boldsymbol{A}}_{\bar{n}} - \boldsymbol{K}_e\bar{\boldsymbol{C}}_{o\bar{n}})\tau} d\tau \cdot \boldsymbol{K}_e \end{aligned} \tag{31}$$

The sampling frequency of the controller, $1/T$, is 40 [kHz], and the other parameters are listed in Tables 1 and 2. The parameters of the Kalman filter are determined experimentally to be optimal values. Figure 11 shows the pole placement of the system. The pole placement is determined in order to provide as much damping as is possible when the DSP is used. The poles of the acoustic space are shown in square of the right side, and the poles of the vibration board are shown in the left side.

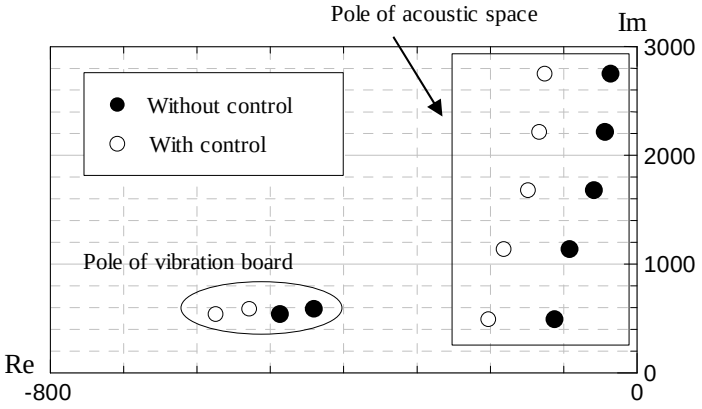

Figure 11 – Pole placement of the proposed system

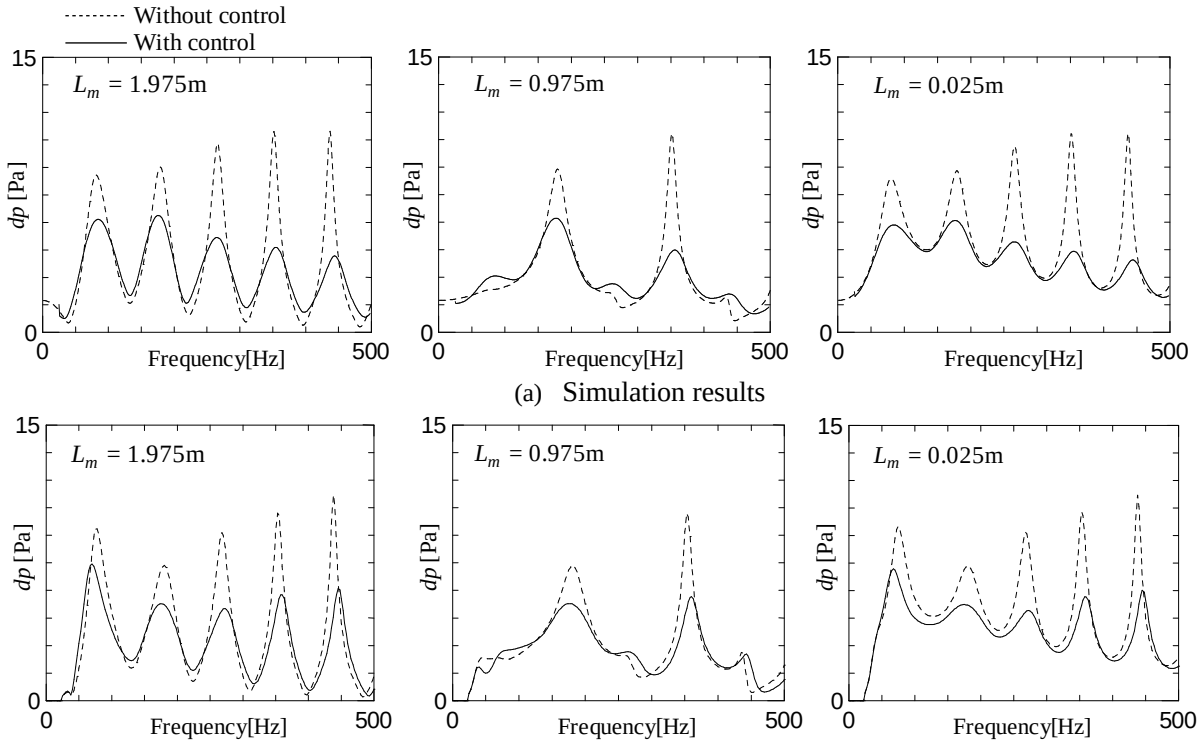

(a) Simulation results

(b) Experimental results

Figure 12 – Control results

5.2 Control Results

The control results obtained using the proposed control method are shown in Fig. 12. The dotted lines indicate the results without control, and the solid lines indicate the results with control. The frequency response of the sound pressure is measured at the microphone (A, B, C). The control effect by the simulation using Eq. (17) is shown in Fig. 12(a). The peak amplitude around the resonance frequency is reduced by the control at each microphone position. The first-order peak at approximately 80 Hz includes three modes (the bottom three poles shown in Fig. 11) and the second- and higher-order peaks are modes of the acoustic space. Moreover, the control results for microphone C (observation point) are better than those for other points because the estimation error of the state variables is the smallest. On the other hand, the experimental results are shown in Fig. 12(b). The peak amplitude around the resonance frequency is reduced, in the same manner as the simulation results. We were not able to obtain greater damping due to the limit of the calculation speed of the DSP. However, it is possible to enhance the control performance by improving the experimental equipment or the control method. Based on the above considerations, the control effect of the proposed control method is confirmed.

6. CONCLUSIONS

In order to design a model-based noise control system and perform noise control for an entire space, we modeled a coupled system of a one-dimensional acoustic space and a loudspeaker as a concentrated mass model. We designed a model-based control system using the proposed model and conducted model reduction using modal analysis to reduce the computation time of the controller. We performed a pressure measurement experiment in a one-dimensional acoustic space in order to confirm the validity of the analysis model. As a result, numerical results obtained using the proposed model and the experimental results were in good agreement in the low-frequency region. Furthermore, we performed a noise control experiment in order to confirm the control effect. The peak amplitude of the sound pressure around the resonance frequency was reduced in the entire acoustic tube. Based on the above considerations, the validity and effectiveness of the proposed control system was confirmed. In the future, we intend to further improve the model, including the damper of the acoustic space, and to realize noise control in higher-dimensional acoustic space.

REFERENCES

1. Fuller, C.R., Elliott, S.J., and Nelson, P.A., Active Control of Vibration (1997), p.91-113, ACADEMIC PRESS.
2. Fumiyasu, K., Masahide, O., and Kazuhisa, K., Active Noise Control System for Engine Booming Noise, Panasonic Technical Journal, Vol.54, No.4 (2009), pp.49-54 (in Japanese).
3. Toshiya, S., and Daisuke, Y., Active modal control of sound fields by finite element modeling and H_∞ control theory, Acoustica science and technology, Vol.23, No.6 (2002), pp.313-322.
4. Hiroshi, S., Yoshihiro, M., Sekiya K., and Itsuro, K., Feedback Active Noise Control with Multiple Control Sources based on Modal Analysis, Transactions of the Japan Society of Mechanical Engineers, Series C, Vol.65, No.633 (1999), pp.1849–1856 (in Japanese).
5. Satoshi, I., Takahiro, K., and Kenichiro M., Nonlinear Pressure Wave Analysis by Concentrated Mass Model (1st Report, Suggestion and Validity Verification of Analytic Model), Jounal of System Design and Dynamics, Vol.3, No.5 (2009), pp.827-840.
6. Takeshi, I., Principles of Acoustic Engineering (1957), p.527, CORONA PUBLISHING CO., LTD. (in Japanese).
7. Karl, B., and Gerhard, S., KALMAN-BUCY FILTERS (1989), p.301, ARTECH HOUSE, INC.
8. Katsuhiko, O., MODERN CONTROL ENGINEERING (THIRD EDITION) (1997), p.825, p.793-795, Prentice-Hall, Inc.
9. Yoshihisa, I., and Masasuke, S., Stability of systems using digital controller based on multi-step methods, System and Control, Vol.29, No.11 (1985), pp.749-757 (in Japanese).